Virology 527 (2019) 57–63

Contents lists available at ScienceDirect

Virology

journal homepage: www.elsevier.com/locate/virology

The role of side tail fibers during the infection cycle of phage lambda

Jingwen Guan[a,b,c], David Ibarra[b], Lanying Zeng[a,b,c,*]

[a] Molecular and Environmental Plant Science, Texas A&M University, College Station, TX 77843, USA
[b] Department of Biochemistry and Biophysics, Texas A&M University, College Station, TX 77843, USA
[c] Center for Phage Technology, Texas A&M University, College Station, TX 77843, USA

ARTICLE INFO

Keywords:
Bacteriophage λ
Side tail fiber
Failed infection
Phage DNA ejection
Cellular decision-making

ABSTRACT

Bacteriophage λ has served as an important model for molecular biology and different cellular processes over the past few decades. In 1992, the phage strain used in most laboratories around the world, thought of as λ wild type, was discovered to carry a mutation in the *stf* gene which encodes four side tail fibers. Up to now, the role of the side tail fibers during the infection cycle, especially at the single-cell level, remains largely unknown. Here we utilized fluorescent reporter systems to characterize the effect of the side tail fibers on phage infection. We found that the side tail fibers interfere with phage DNA ejection process, most likely through the binding with their receptors, OmpC, leading to a more frequent failed infection. However, the side tail fibers do not seem to affect the lysis-lysogeny decision-making or lysis time.

1. Introduction

As the most abundant organisms in the world, bacteriophages (simply phages) are viruses that infect bacteria. Phage λ was discovered in 1951 by Esther Lederberg (Lederberg, 1951). Ever since its discovery, phage λ has become one of the most comprehensively studied phage systems and serves as paradigms of different biological processes, such as regulation of gene expression, mechanisms of recombination, and cell-fate decision-making (Hendrix, 1983; Ptashne, 1986; Oppenheim et al., 2005; Hendrix and Casjens, 2006). To start an infection, phage λ first carries out the interaction with the host cell through its tail fiber binding to the receptor on the host cell. Subsequently, λ DNA is ejected into the cell, followed by a decision to enter either of two distinct pathways, lysis or lysogeny. In the lytic pathway, λ replicates its DNA and produces new phages, resulting in cell lysis to release about a hundred progeny virions. Alternatively, in the lysogenic pathway, λ establishes the dormant state by integrating its genome into the host chromosome, and existing as a quiescent prophage (Ptashne, 1986; Court et al., 2007).

The phage λ used in most laboratories around the world, which has been thought of as wild-type λ (λWT) is actually not the original strain that was isolated from a prophage in *E. coli* strain K-12 in 1951 (Lederberg, 1951). It is a mutant strain derived from a cross between a λ strain in use in Pasadena and another strain in use in Paris, and later referred to as lambda *PaPa* (λ*PaPa*) (Hendrix and Duda, 1992). The real wild type strain is referred to as Ur-lambda (Ur-λ). Compared with λWT (or λ*PaPa*) which only has a short tail fiber at the tail tip, Ur-λ virions have additional four long, thin side tail fibers that extend from the side of the tail tip (Hendrix and Duda, 1992; Casjens and Hendrix, 2015). The absence of the side tail fibers from λWT is the result of a frameshift mutation (a deletion of cytosine) in the side tail fiber (*stf*) gene in λWT genome sequence (Hendrix and Duda, 1992). Without those side tail fibers, λWT produces larger plaques on cell lawn, which makes them more suitable for genetics studies in the early days (Casjens and Hendrix, 2015; Gallet et al., 2011). Although the side tail fibers are not essential for λ plaque formation, they greatly accelerate the rate of adsorption onto the host cell surface by ~7.4 fold (Shao and Wang, 2008). That is because in addition to the binding of the λ receptor, LamB, on the outer membrane of *E. coli* by the tail fiber gpJ protein, the extra side tail fibers on Ur-λ can bind to another host outer membrane protein OmpC (Hendrix and Duda, 1992; Hendrix and Casjens, 2006). Moreover, the side tail fibers presumably slow down the diffusion of Ur-λ through the top agar layer, resulting in the smaller plaque size (Gallet et al., 2011). However, how the side tail fibers affect phage lambda infection remains largely unknown.

In this study, we characterize the infection cycle of Ur-λ at the single-cell level using fluorescent reporter systems (Trinh et al., 2017). By following the phage infection, we reveal the differences between Ur-λ and λWT such as the lysogenic response to the number of infecting phages and the failed infection frequency.

* Corresponding author at: Department of Biochemistry and Biophysics, Texas A&M University, College Station, TX 77843, USA.
E-mail address: lzeng@tamu.edu (L. Zeng).

https://doi.org/10.1016/j.virol.2018.11.005
Received 16 August 2018; Received in revised form 7 November 2018; Accepted 8 November 2018
Available online 18 November 2018
0042-6822/

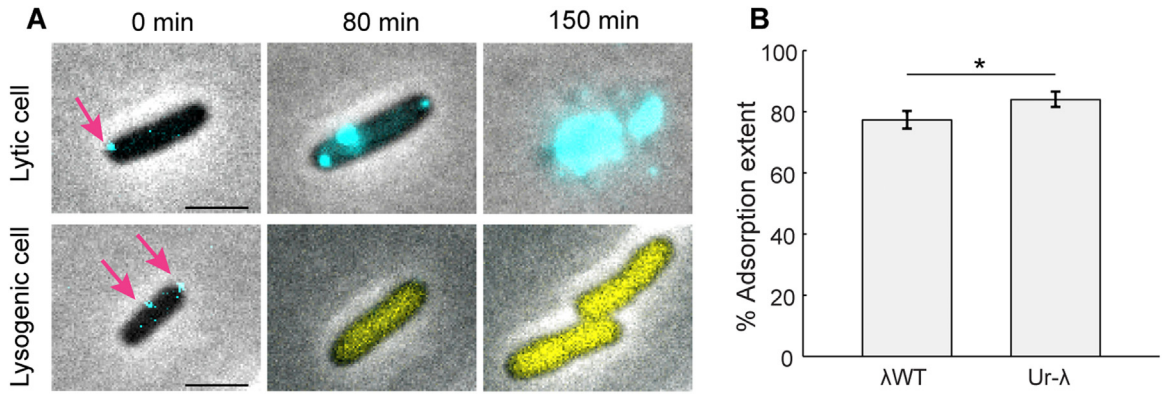

Fig. 1. Visualization of phage λ decision-making and the adsorption assay in single cells. (A) Top: a representative lytic cell was infected by one λ phage at 0 min (blue dot, pointed by magenta arrow), and subsequently gpD-mTurquoise2 fluorescence (blue) developed over time, followed by cell lysis at 150 min. Bottom: a representative lysogenic cell was infected by two λ phages at 0 min (blue dots, pointed by magenta arrows), and subsequently *cI*-mKO2 fluorescence (yellow) developed over time, followed by cell growth and cell division. Scale bar denotes 2 μm. (B) Ur-λ has a higher adsorption extent (84.0 ± 2.2%) than λWT (77.3 ± 2.6%) at the single-cell level. *: $p < 0.05$. Error bars denote standard error of the mean (SEM).

2. Results

2.1. The side tail fibers increase the adsorption of Ur-λ

In order to characterize the infection of Ur-λ at the single-cell level, we took advantage of our previously established fluorescent reporter system to visualize infecting phage particles and report the lysis-lysogeny pathways under the fluorescence microscope (Trinh et al., 2017). Briefly, fluorescent protein gene *mTurquoise2* was translationally fused to λ*D* gene, encoding λ capsid decoration protein, which allows for the visualization of the infecting phages and reporting the lytic pathway. Meanwhile, the lysogenic pathway is reported by fluorescent protein mKO2 which was transcriptionally fused after λ*cI* gene, whose product is required for lysogenic establishment and maintenance (Fig. 1A). These two modifications result in the λWT reporter phage (λ_{LZ1502}, λ*D-mTurquoise2 cI*$_{857}$*-mKO2 bor::Kan*^{R}). Subsequently, through the genetic recombination based on the method in Shao and Wang (2008), we restored the functional λ*stf* gene back into the genome of the above λWT reporter phage and sequenced the entire *stf* gene and confirmed the insertion of an additional cytosine at positions 20833 to 20835 relative to λWT genome sequence. Eventually, an Ur-λ phage with the same dual-color reporter system was constructed: λ_{LZ1636}, λ*D-mTurquoise2 stf* + *cI*$_{857}$*-mKO2 bor::Kan*^{R}. Thereafter, we performed single-cell infection experiments with both Ur-λ and λWT reporter phages.

We first compared the abilities of Ur-λ and λWT to adsorb onto the host cells. As reported in the literature (Hendrix and Duda, 1992) and our previous bulk measurements (Cortes et al., 2017), Ur-λ has an increased adsorption rate compared with λWT. To examine the adsorption at the single-cell level, we followed our standard single-cell infection protocols (Trinh et al., 2017; Zeng et al., 2010). Briefly, *E. coli* host cells were mixed with Ur-λ or λWT phages, followed by an incubation on ice for 30 min to allow phages adsorb onto host cells and an additional incubation at 35 °C for 5 min to trigger phage DNA ejection. The infection mixture was then transferred onto an agarose pad of medium for imaging (See details in Section 4). From the images, by calculating the ratio of the number of fluorescent phages attached on the cell surface to the number of all phages shown in the frame, we were able to quantify the adsorption extents of both phages. 84.0 ± 2.2% (6746 attached phages out of 8034 total phages in 11 experiments) of Ur-λ phages were adsorbed on *E. coli* host cells, significantly more than 77.3 ± 2.6% (6365 out of 8239 phages in 9 experiments) of λWT phages (Mann-Whitney *U*-test, $p < 0.05$) (Fig. 1B). This confirms that the side tail fibers help Ur-λ to encounter the host for infection.

2.2. Ur-λ has a higher chance of failure in the infection

We next sought to determine whether the adsorbed phage can successfully infect the cell. A failed infection event is marked when a cell fails in establishing either lytic or lysogenic pathway even with phages attached (Fig. 2A). It was reported that phage lambda fails around 20–25% under the standard infection condition (Zeng et al., 2010; Mackay and Bode, 1976). With the side tail fibers, we expect that Ur-λ may have a reduced failed infection frequency as those side tail fibers could possibly stabilize the adsorption and facilitate phage DNA ejection process. However, to our surprise, Ur-λ exhibited a much higher failed infection frequency (42.0 ± 1.6%, 261 out of 606 cells in 11 experiments) than λWT (29.2 ± 1.8%, 173 out of 593 cells in 9 experiments) at MOI = 1 (multiplicity of infection, the number of infecting phages for each cell) ($p < 0.001$) (Fig. 2B). This phenomenon holds true for higher MOIs (Fig. 2C).

Phage λ tail fiber gpJ directly interacts with the receptor LamB for infection (Wang et al., 1998). To rule out the possibility that our Ur-λ phage possesses a deficient tail fiber gpJ due to any mutations in the sequence of gene *J*, leading to the higher failed infection frequency, we sequenced the *J* gene of the unlabeled and fluorescently labeled λWT and Ur-λ phages and confirmed that the sequences of the *J* gene in all four phages are identical to the *J* gene sequence reported in Sanger et al. (1982) (RefSeq accession no. NC_001416.1).

The failed infection could be due to unsuccessful or incomplete ejection of phage DNA into the cytoplasm (failed ejection), or inability to finish either the lytic or lysogenic pathway with a successful DNA ejection (failed establishment). Our previous work showed that the former case is the dominant cause for the failed infection (Shao et al., 2015). Here, to compare Ur-λ with λWT, we utilized our established SeqA-DNA binding reporter system to visualize ejected phage DNA inside the cell (Shao et al., 2015). Briefly, we prepared *E. coli* host with *dam*$^-$ mutation and *seqA-mKO2* fusion on its genome (Trinh et al., 2017). Phage λ DNA is known to be partially methylated when phages are propagated in wild-type *E. coli* cells (Szyf et al., 1984). Once a successful ejection of phage DNA happens, the uniformly distributed SeqA-mKO2 protein will bind to the ejected DNA forming a fluorescent focus. The successful ejection is indicated by the formation of SeqA foci, and when the cell is followed by lytic fluorescence signal (lytic cell) or *cI*-mKO2 signal followed by cell division (lysogenic cell), this marks as successful infection. In contrast, the failed ejection was indicated when SeqA-mKO2 protein remains as uniform distribution inside the cell with fluorescent phage(s) attached on the cell surface. At MOI = 1, 38.4 ± 3.0% (135 out of 352 cells in 10 experiments) of Ur-λ phages failed to eject their DNAs into the cells, whereas λWT phages remained

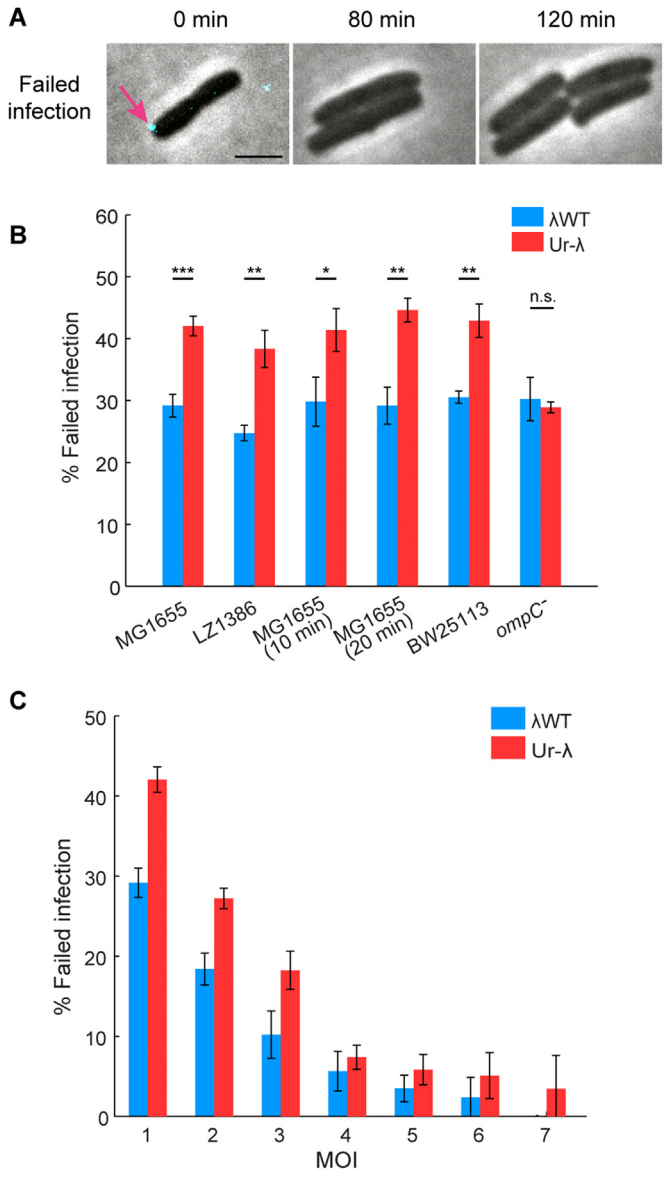

Fig. 2. The side tail fibers of Ur-λ contribute to failure in the infection. (A) A representative cell showing the failed infection event by one phage λ (blue dot, pointed by magenta arrow at 0 min). The cell did not show either gpD-mTurquoise2 or *cI*-mKO2 fluorescence over time and divides like uninfected cells, indicating that the phage failed to establish either the lytic or lysogenic development. Scale bar denotes 2 μm. (B) The failed infection frequencies of Ur-λ and λWT at MOI = 1 in different *E. coli* strains. Ur-λ shows a higher failed infection frequency in ejecting phage DNA than λWT in MG1655, LZ1386, MG1655 with 10 min treatment (see treatment details in the main text), MG1655 with 20 min treatment, and BW25113. In *ompC*⁻ strain, Ur-λ has a similar failed infection frequency as λWT. *: $p < 0.05$, **: $p < 0.01$, ***: $p < 0.001$, and n.s.: not significant. λWT: blue, Ur-λ: red. (C) The failed infection frequency of λWT and Ur-λ as a function of MOI in MG1655. For both phages, the failed infection frequency decreases with MOI. Ur-λ (red) fails more frequently than λWT (blue) at different MOIs. In all plots, error bars denote standard error of the mean (SEM).

a lower frequency of 24.7 ± 1.3% (96 out of 388 cells in 9 experiments) ($p < 0.01$) (Fig. 2B). These numbers are comparable to the failed infection frequencies measured above, which confirms that the higher failed infection frequency of Ur-λ is mainly caused by failed DNA ejection rather than failed establishment of cell fate. This leads to our hypothesis that the side tail fibers of Ur-λ might be involved in the process of phage DNA ejection.

We then speculated whether our single-cell infection protocol artificially increased the failed infection frequency of Ur-λ. The current picture of phage lambda infection is that phage first follows a free 3D diffusion in solution. When it lands on the cell, the 3D diffusion will transit into a 2D motion on the cell surface. Finally, the phage's tail fiber gpJ irreversibly binds to a LamB receptor, preferentially at cell poles or midcell (future pole) positions for DNA ejection (Rothenberg et al., 2011; Edgar et al., 2008). This was achieved by a relaxed liquid condition of phage lambda tail fiber gpJ to find the LamB receptor on the cell surface. However, in our standard protocol for the single-cell studies, phages and cells were first mixed in a tube and incubated on ice for 30 min, followed by another 5 min incubation at 35 °C to trigger phage DNA ejection. After that, the phage-cell mixture was transferred onto a thin 1.5% agarose pad and covered by a coverslip for subsequent microscopy imaging. Consequently, it is possible that under our experimental conditions, Ur-λ has not found a LamB receptor at its preferential positions on the cell to accomplish DNA ejection before the phage-cell mixture was transferred onto the agarose pad. In addition, those Ur-λ phages which have already arrived at a LamB receptor site, the tail fiber gpJ might not be able to perfectly interact with LamB due to the agarose pad, leading to the failed DNA ejection. In order to ensure that phages have sufficient time to search for the receptor sites and accomplish DNA ejection, we performed the same single-cell experiments but extended the triggering time for phage DNA ejection at 35 °C from 5 min to 10 min and 20 min. Ur-λ still failed more frequently than λWT, with 41.4 ± 3.4% (48 out of 116 cells) versus 29.8 ± 4.0% (17 out of 57 cells) and 44.2 ± 1.9% (58 out of 130 cells) versus 29.2 ± 3.0% (28 out of 96 cells) for 10 min and 20 min incubation at MOI = 1 respectively (Fig. 2B). This indicates that our standard single-cell experimental procedure does not artificially give rise to the higher failed infection frequency of Ur-λ.

2.3. The interaction between the side tail fibers and their receptors contributes to the failed infection

We next asked how the presence of side tail fibers causes the high frequency of failed infection for Ur-λ. It has been reported that the side tail fibers of phage λ can recognize an outer membrane protein OmpC on *E. coli* (Gallet et al., 2011; Montag et al., 1989). Once phage λ attaches on *E. coli* host, its tail fiber searches for LamB receptors on the cell surface to initiate DNA ejection. Given that OmpC proteins are located at random locations and tend to move freely on *E. coli* outer membrane (Begg and Donachie, 1984; Begg, 1978), it is possible that by interacting with OmpC receptor, the phage side tail fibers indirectly impede the binding of phage tail fiber gpJ to LamB, which has also been shown to be mobile (Gibbs et al., 2004), for DNA ejection. In order to test this hypothesis, we used an *E. coli ompC*⁻ strain (JW2203, *ΔompC768::kan*^{R}) to determine the effect of OmpC on phage failed infection frequency. We also used *E. coli* BW25113, the parent strain of JW2203, as a control. Through the same single-cell experiments outlined in the previous section, we found that the failed infection frequency of Ur-λ decreased significantly from (42.9 ± 2.7%, 142 out of 331 cells at MOI = 1 in 4 experiments) in BW25113 host to 28.9 ± 0.9% (63 out of 218 cells at MOI = 1 in 3 experiments) in *ompC*⁻ host ($p < 0.01$), while λWT kept a similar failed infection frequency in BW25113 to that in *ompC*⁻ host (30.5 ± 1.0%, 127 out of 416 cells at MOI = 1 in 4 experiments, versus 30.2 ± 3.5%, 75 out of 248 cells at MOI = 1 in 3 experiments, $p = 0.62$) (Fig. 2B). The data confirm the hypothesis that the interaction between the side tail fibers and their receptors on the host surface is involved in interfering with the Ur-λ infection process. When this interaction is removed, Ur-λ is able to restore the higher frequency of successful infection.

2.4. The side tail fibers make a stronger binding Ur-λ on the cell surface

In addition to the failed infection, we examined dark infection,

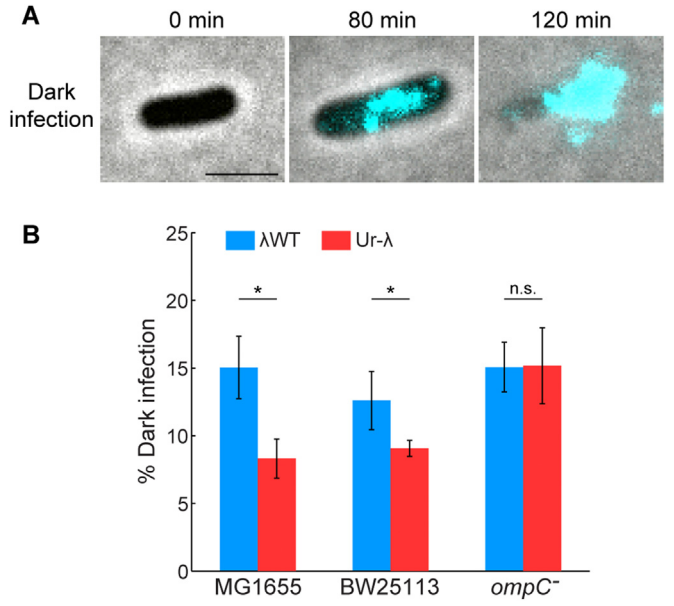

Fig. 3. The side tail fibers enhance the adsorption of Ur-λ on the host cell. (A) A representative cell showing the dark infection event. No fluorescent phage particle was detected on the cell surface. However, the cell showed lytic reporter signal over time, followed by cell lysis at 120 min. Scale bar denotes 2 μm. (B) The dark infection frequencies of Ur-λ are lower than those of λWT at MOI = 1 in wild-type *E. coli* MG1655 and BW25113. In *ompC*⁻ strain, Ur-λ shows a similar dark infection frequency compared with λWT. *: $p < 0.05$, and n.s.: not significant. λWT: blue, Ur-λ: red. Error bars denote standard error of the mean (SEM).

indicated by successful infection with cells ending up with lytic or lysogenic fates even without any fluorescent phage particles detectable on the cell surface (Fig. 3A). It is possibly a result of phages shearing off from the host cells after ejecting their DNA, likely caused by the performance of the experiments (Zeng et al., 2010). Or some of the dark infection cells could be the daughter cells dividing from the initial infected cells before imaging (Zeng et al., 2010). The dark infection frequency is calculated as the ratio of the number of dark infections to the total cell number of MOI = 1 plus the number of dark infections, based on the assumption that all dark infection cells are mostly infected by only one phage. We expect Ur-λ having a reduced dark infection frequency, because besides the binding by the tail fiber to the main receptor LamB, its side tail fibers provide an additional binding to OmpC proteins on the host cell surface, resulting in a tighter adsorption. Our single-cell studies showed that Ur-λ indeed had a lower dark infection frequency (8.3 ± 1.4%, 66 out of 728 cells at MOI = 1 in 11 experiments) compared with 15.0 ± 2.3% (105 out of 593 cells at MOI = 1 in 9 experiments) of λWT ($p < 0.05$) when infecting MG1655 (Fig. 3B). On the other hand, upon infection of *ompC*⁻ host, Ur-λ exhibited an indistinguishable dark infection frequency (15.2 ± 2.8%, 39 out of 218 cells at MOI = 1 in 3 experiments), compared with λWT (15.1 ± 1.8%, 44 out of 248 cells at MOI = 1 in 3 experiments) ($p = 0.49$) (Fig. 3B). As a control, Ur-λ still had a lower dark infection frequency than λWT in BW25113 (9.1 ± 0.6%, 33 out of 331 cells at MOI = 1 in 4 experiments, versus 12.6 ± 2.2%, 60 out of 416 cells at MOI = 1 in 4 experiments, $p < 0.05$, Fig. 3B). These results suggest that the side tail fibers make a stronger adsorption of Ur-λ on cell surface through binding to OmpC, which leads to less dark infection.

2.5. The effect of the side tail fibers on Ur-λ post-infection

We first characterized the effect of the side tail fibers on Ur-λ DNA ejection time, using the aforementioned phage DNA labeling system. For phage λWT, it was reported that the DNA ejection is completed with a mean of 5 min ranging from 1 min to 20 min with great cell-to-cell variability (Van Valen et al., 2012). Our previous work using SeqA-DNA reporter system also showed that approximately 95% of phage DNAs appeared inside the cell within 5 min following phage infection (Shao et al., 2015; Guan et al., 2017). Here, by examining the appearance time of fluorescently labeled phage DNA inside the cell, we did not observe a significantly different distribution between Ur-λ and λWT (Fig. 4A). 79.7 ± 5.1% (118 out of 148 cells in 10 experiments) of Ur-λ DNA fluorescence foci showed up within 6 min, comparable to 85.2 ± 4.0% (195 out of 229 cells in 9 experiments) for λWT ($p = 0.35$). Considering the higher failed infection frequency of Ur-λ, the data further imply that the side tail fibers might not be able to promote Ur-λ to eject its DNA in a faster, more successful and synchronized manner.

We next sought to investigate whether Ur-λ exhibits different cellular decision-making behaviors from λWT. We first examined the lysogenization response to MOI in bulk. In the bulk assay, MOI is referred to as API (average phage input), the ratio of phage concentration in pfu (plaque forming units) to cell concentration in cfu (colony forming units) (Kourilsky, 1973). As expected, Ur-λ increased with API, but exhibited a higher lysogenization frequency than λWT. This higher lysogenization frequency might be resulted from the higher adsorption extent of Ur-λ giving rise to a higher effective API. In addition, Ur-λ followed the same $N \geq 2$ Poisson distribution as λWT, indicating that the regulation for lysis-lysogeny decision-making remains the same (Fig. 4B). This is reasonable since *stf* gene lies in the late operon and is only turned on during the late stage of infection when a lytic decision has been made. Furthermore, the two reporter phage strains lysogenized like their corresponding unlabeled strains (Fig. 4B), suggesting that the genetic modification for the fluorescent reporter does not affect the lysogenization and adsorption behavior. We then moved to test whether Ur-λ lysogenizes the cell in the same manner as λWT at the single-cell level. We found that the lysogenization probability of Ur-λ increased with MOIs, similar to λWT. At MOI = 1, Ur-λ and λWT exhibited a similar lysogenization frequency since Ur-λ shares the same lysis-lysogeny decision-making circuity as λWT as expected. However, at MOI > 1, Ur-λ phages lysogenize the cell slightly less frequently than λWT (Fig. 4C). This is probably due to the higher failed infection frequency (42.0%) of Ur-λ than that of λWT (29.2%) resulting in a lower effective MOI of Ur-λ than that of λWT.

Furthermore, we examined another important downstream effect, lysis time. Lysis time is an important phage trait, which often defines phage fitness (Shao and Wang, 2008). It was reported that phage λ with and without the side tail fibers both had a lysis time of 52.3 min in bulk (Shao and Wang, 2008). Here, our single-cell data showed that Ur-λ shared a similar distribution of lysis time to λWT (Fig. 4D) with the average lysis time of 112 min (898 lytic cells) for Ur-λ and 104 min (895 lytic cells) for λWT respectively. Note that our growth condition is very different from that in Shao and Wang (2008), where a rich medium LB was used as the growth medium and the cell-phage mixtures were incubated in culture flasks with good aeration (Shao and Wang, 2008). Whereas, in this study, we used M9 minimal medium for cell growth in order to reduce the fluorescence background under the microscope. Moreover, the cell-phage mixtures were placed under an agarose pad without shaking. In addition, the lysis time of λWT in this study agrees well with a previous study under a similar growth condition (Trinh et al., 2017).

3. Discussion

With the advancement of high-resolution microscopy, researchers can examine biological systems at unprecedented levels. It turned out that phage lambda has been discovered to have quite surprising behaviors than previously thought (Trinh et al., 2017; Cortes et al., 2017; Zeng et al., 2010; Van Valen et al., 2012; Shao et al., 2018). For example, lambda ejects its DNA into its host cell with great cell-cell

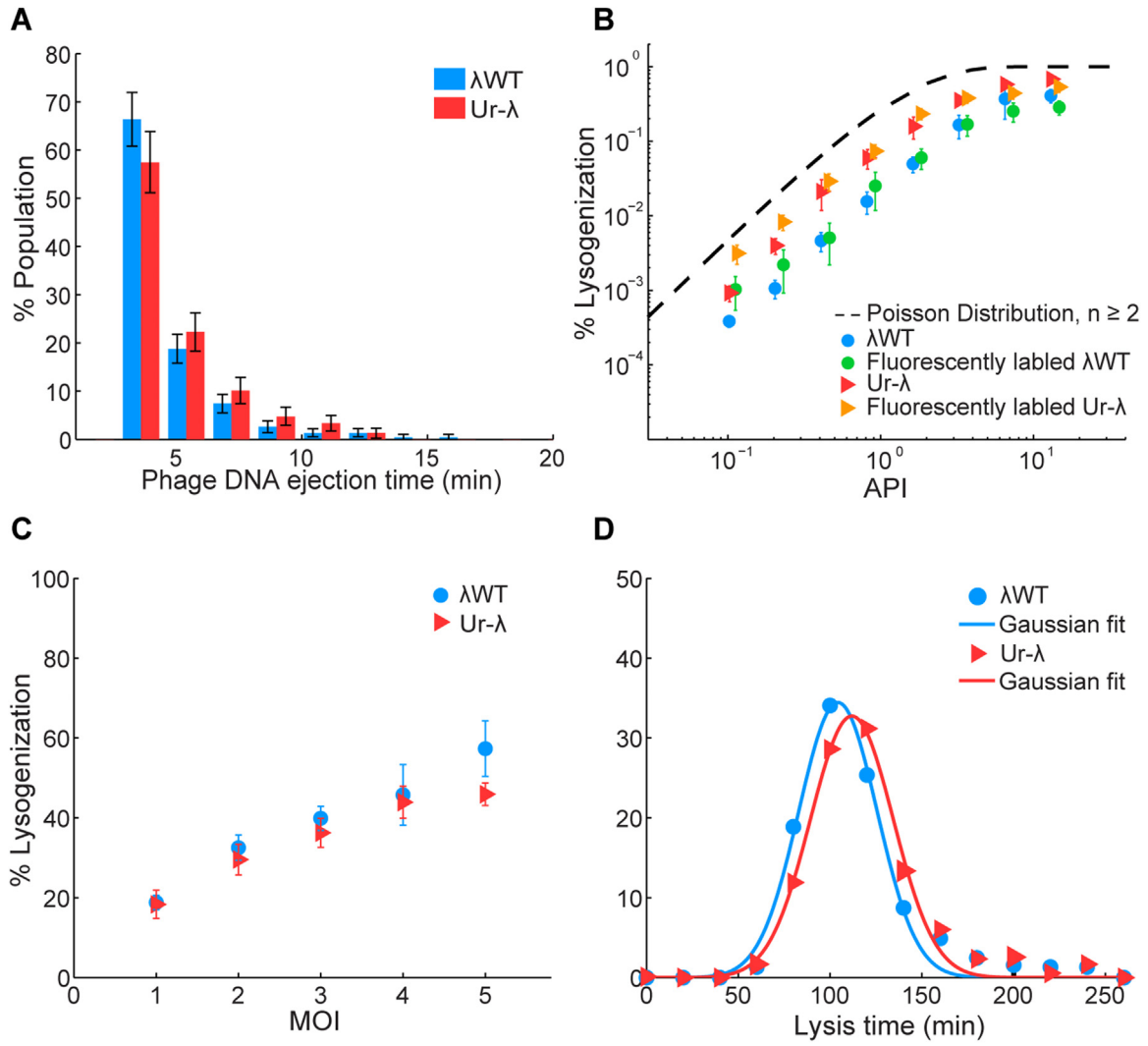

Fig. 4. The effect of the side tail fibers on Ur-λ post-infection. (A) Histogram of λWT and Ur-λ phage DNA spot appearance time. 85.2% of λWT DNA fluorescence foci appear within the first 6 min in the movies, while 79.7% of Ur-λ DNA foci appear within the same time frame. λWT: blue, Ur-λ: red. Data are represented as mean ± SE (based on counting error). (B) Lysogenization frequency of λWT and Ur-λ as a function of API in bulk. All phage strains follow the theoretical prediction of Poisson distribution of n ≥ 2 (black dashed line). Ur-λ (red triangles) has higher lysogenization frequencies than λWT (blue circles) at different APIs. Fluorescent Ur-λ (orange triangles) and fluorescent λWT (green circles) lysogenize similarly as their corresponding unlabeled phage strains. Error bars denote standard error of the mean (SEM). (C) Lysogenization frequency of λWT and Ur-λ as a function of MOI at the single-cell level. The lysogenization frequencies of both phages increase with MOI. At MOI = 1, Ur-λ has a similar lysogenization frequency (18.3 ± 3.5%) to that of λWT (18.8 ± 1.8%). At MOI > 1, Ur-λ exhibits slightly lower lysogenization frequencies. Error bars denote standard error of the mean (SEM). λWT: blue circles, Ur-λ: red triangles. (D) Distribution of lysis time for λWT and Ur-λ lytic cells. Ur-λ (red triangles) and λWT (blue circles) show similar distributions of lysis time, with an average lysis time of 112 min and 104 min respectively. Experimental data were well fitted to a Gaussian function (lines).

Table 1
Bacterial strains, phages and plasmids used in this work.

Bacterial strains, plasmids, and phages		
Strain Name	**Relevant Genotype/Comments**	**Source/Reference**
Bacterial strains		
MG1655	*sup*^{0}, Wild type *E. coli*	Lab collection
BW25113	The parent strain of JW2203	Lab collection
JW2203	*ΔompC768::kan*^{R} (CGSC#9781)	(Baba et al., 2006)
LZ1386	MG1655 *seqA-mKO2 Δdam::Kan*^{R} *Cm*^{R}	(Trinh et al., 2017)
Phage strains		
λ_{LZ613}	λ*cI*$_{857}$ *bor::Kan*^{R}, referred to as λWT or λ*PaPa*	(Shao et al., 2015)
λ_{LZ610}	λ*cI*$_{857}$ *stf+ bor::Kan*^{R}, referred to as Ur-λ	This work
λ_{LZ1367}	λ*D-mTurquoise2 cI*$_{857}$*-mKO2 bor::Cm*^{R}, referred to as λWT-reporter	(Trinh et al., 2017)
λ_{LZ1636}	λ*D-mTurquoise2 stf+ cI*$_{857}$*-mKO2 bor::Kan*^{R}, referred to as Ur-λ-reporter	This work
Plasmids		
pZE1-*ΔJ-Cm*^{R}*-stf*	Contains part of *J* and *Cm*^{R} replacing the region between *J* and *orf314*, *Cm*^{R} *Amp*^{R}	(Shao and Wang, 2008)
pZE1-*J-stf+*	Contains part of *J* and functional *stf*, *Amp*^{R}	(Shao and Wang, 2008)

variability (Van Valen et al., 2012), which can be due to the mobility of the encapsidated phage DNA (Evilevitch, 2018). The timing of phage lambda DNA ejection greatly affects the downstream lysis-lysogeny decision making and development of the phage (Trinh et al., 2017; Cortes et al., 2017). We would expect that the four side tail fibers of Ur-λ facilitate the DNA ejection process due to their extra binding on the cell surface. However, we found Ur-λ exhibited more frequent failed DNA ejection. The DNA ejection happens when phage lambda tail fiber gpJ interacts LamB receptor. So, it seems that the binding of side tail fibers to OmpC receptor disturbs the optimal interaction between gpJ and LamB. This raised the question why the real wild type lambda even needs the four side tail fibers. We know that with the four side tail fibers, Ur-λ can adsorb to the host at a much faster rate and higher extent. Therefore, Ur-λ can have more efficient infection even when each individual phage might fail more frequently compared to λWT. This is probably why Ur-λ would still be a phage with higher fitness (Shao and Wang, 2008).

4. Materials and methods

4.1. Bacterial strains, plasmids and phages

All bacterial strains, plasmids and phages used are listed in Table 1. *E. coli* wild-type strain MG1655 was used as the host strain for bulk lysogenization assay and normal phage movies. *E. coli* strain LZ1386 (MG1655 *seqA-mKO2* Cm^R *Δdam::*Kan^R) used for tracking phage DNA ejection was obtained from our recent work (Trinh et al., 2017). *E. coli* strain defective in OmpC expression (JW2203, *ΔompC768::kan*) was obtained from the Keio collection (CGSC#9781) (Baba et al., 2006). *E. coli* BW25113 was used as a control strain to determine the effect of OmpC on phage infection. Wild-type phage λ ($λ_{LZ613}$, λ*cI*$_{857}$ *bor::*Kan^R) and wild-type phage λ reporter strain ($λ_{LZ1367}$, λ*D-mTurquoise2 cI*$_{857}$*-mKO2 bor::*Cm^R) were constructed previously (Trinh et al., 2017; Shao et al., 2015). Ur-λ ($λ_{LZ610}$, λ*cI*$_{857}$ *stf+ bor::*Kan^R) and Ur-λ reporter strain ($λ_{LZ1636}$, λ*D-mTurquoise2 stf+ cI*$_{857}$*-mKO2 bor::*Kan^R) were produced by restoring the frameshift mutation present in the side tail fiber gene (*stf*) back into the genome of λWT and λWT reporter strain respectively through site-directed mutagenesis and recombination as described in (Shao and Wang, 2008). Plasmids pZE1-*ΔJ-*Cm^R*-stf* and pZE1-*J-stf+* were received as gifts from Ryland Young, Texas A&M University. All phages were produced through the heat-induction of lysogens, followed by a standard CsCl purification procedure following the protocol described in Zeng and Golding (2011).

4.2. Bulk lysogenization assay

As described in previous work (Trinh et al., 2017; Zeng et al., 2010), host *E. coli* MG1655 cells were diluted 1:100 from an overnight culture and grown in LBMM at 37 °C, 265 rpm, until an OD_{600} of ~0.4. The cells were collected by centrifugation (1000 × *g* for 10 min at 4 °C) and concentrated 10 × in pre-chilled fresh LBMM. Phages were diluted from original stocks to reach a maximal API of ~10, and then proceeded into a 2-fold series of dilution until 2^{-8}. 20 μL of the cell suspension was infected with 20 μL of phages at different concentrations by incubation on ice for 30 min, followed by another incubation at 35 °C for 5 min to trigger phage DNA ejection. Subsequently, 10 μL of each infection mixture was then added into 1 mL of pre-warmed LBGM (LB + 0.2% glucose + 10 mM $MgSO_4$), and incubated with shaking at 265 rpm at 30 °C for 45 min. The samples were then properly diluted with 1 × PBS and spread onto LB + *Kan* or LB + *Cm* plates to allow 100–200 lysogens to grow at 30 °C for overnight.

4.3. Single-cell infection assay

1 mL of host cell MG1655 was grown in M9 minimal medium (11.3 g/L M9 salts, 1 mM $MgSO_4$, 0.5 μg/mL thiamine HCl, 0.1% casamino acids, 100 μM $CaCl_2$) supplemented with 0.4% maltose (M9M) at 37 °C for overnight. The overnight culture was subsequently diluted 1:100 into 5 mL of M9M and grown at 37 °C with 265 rpm shaking until OD_{600} of ~0.3. 1 mL of cells were then concentrated by centrifugation at 2000 × *g* for 2 min at room temperature, and re-suspended in ice-cold M9M to OD_{600} of ~3. 10 μL of phage stock was mixed with 10 μL of the resuspended cells to reach an appropriate API, followed by incubation on ice for 30 min and an additional 5 min incubation at 35 °C water bath to trigger phage DNA ejection. The phage-cell mixture was then diluted by 10 fold into 50 μL of M9M at room temperature. 1 μL of the diluted mixture was placed onto a 1.5% agarose pad of M9M (~1 mm thick) until visibly dry (~1 min). A coverslip (No.1, Fisher Scientific) was gently laid over the mixture and the sample was imaged under the fluorescence microscope at 30 °C within a cage incubator (InVivo Scientific, St. Louis, MO). For the phage DNA reporter movies, the same protocol was performed but with the reporter host strain (MG1655 *seqA-mKO2* Cm^R *Δdam::*Kan^R) (Trinh et al., 2017).

4.4. Fluorescence microscopy and imaging

Microscopy was performed on an inverted epifluorescence microscope (Ti-E, Nikon, Tokyo, Japan) using a 100 × objective (Plan Fluo, NA 1.40, oil immersion) with a 2.5 × TV relay lens and standard filter sets. Images were acquired using a cooled EMCCD camera (iXon3 897, Andor, Belfast, United Kingdom). Acquisition was performed using Nikon Elements software. Typically, 16 stages with well-separated cells were selected for each movie. In order to visualize all infecting phages surrounding the cells, a series of 7 z-stack (vertical) images at a spacing of 300 nm were taken for the first frame through the blue (mTurquoise2/CFP, 200 ms exposure) channel. During the time-lapse movie, the sample was imaged every 5 min at the focal plane for 4 h through the channel of the phase contrast (100 ms exposure, for cell recognition), blue (mTurquoise2/CFP, 40 ms exposure, for phage lytic reporter), and yellow (mKO2, 100 ms exposure, for phage lysogenic reporter).

For the phage DNA reporter movies, the first frame of the sample was imaged with 7 z-stacks at a spacing of 300 nm under both blue (mTurquoise2/CFP, 300 ms exposure) and yellow (mKO2, 200 ms exposure) channels to localize infecting phages surrounding the cells and detect phage DNA foci inside the cells. The time-lapse movies were taken at a time interval of 2 min, until the phage DNA foci were not detectable (1 h) due to photobleaching. The images were acquired in phase contrast (100 ms exposure, for cell recognition), blue (mTurquoise2/CFP, 100 ms exposure, for phage lytic reporter) and yellow (mKO2, 200 ms exposure, with a series of 7 z-axis images at a spacing of 300 nm, for phage DNA detection) channels.

4.5. Data analysis

Movie images were analyzed using the cell recognition program Schnitzcell (gift of Michael Elowitz, California Institute of Technology) in the phase-contrast channel. All data analysis was performed in Matlab (The MathWorks, Natick, MA) using our homemade script.

Acknowledgements

We are grateful to Ryland Young for providing the plasmids and strains and generous suggestions. We thank members of the Zeng laboratory for help with the experiments and discussions. This work was supported by the National Institutes of Health (R01GM107597).

Declaration of interest

The authors declare that there is no conflict of interest.

Author Contributions

LZ: Conceptualization, Funding acquisition, Investigation, Supervision, Writing - original draft, Writing - review & editing; JG: Data curation, Formal analysis, Investigation, Writing - original draft, Writing - review & editing; DI: Formal analysis.

References

Baba, T., Ara, T., Hasegawa, M., Takai, Y., Okumura, Y., Baba, M., Datsenko, K.A., Tomita, M., Wanner, B.L., Mori, H., 2006. Construction of Escherichia coli K-12 in-frame, single-gene knockout mutants: the Keio collection. Mol. Syst. Biol. 2 (p. 2006 0008).

Begg, K.J., 1978. Cell surface growth in Escherichia coli: distribution of matrix protein. J. Bacteriol. 135 (2), 307–310.

Begg, K.J., Donachie, W.D., 1984. Concentration of a major outer membrane protein at the cell poles in Escherichia coli. J. Gen. Microbiol. 130 (9), 2339–2346.

Casjens, S.R., Hendrix, R.W., 2015. Bacteriophage lambda: early pioneer and still relevant. Virology 479–480, 310–330.

Cortes, M.G., Trinh, J.T., Zeng, L., Balazsi, G., 2017. Late-arriving signals contribute less to cell-fate decisions. Biophys. J. 113 (9), 2110–2120.

Court, D.L., Oppenheim, A.B., Adhya, S.L., 2007. A new look at bacteriophage lambda genetic networks. J. Bacteriol. 189 (2), 298–304.

Edgar, R., Rokney, A., Feeney, M., Semsey, S., Kessel, M., Goldberg, M.B., Adhya, S., Oppenheim, A.B., 2008. Bacteriophage infection is targeted to cellular poles. Mol. Microbiol. 68 (5), 1107–1116.

Evilevitch, A., 2018. The mobility of packaged phage genome controls ejection dynamics. Elife 7.

Gallet, R., Kannoly, S., Wang, I.N., 2011. Effects of bacteriophage traits on plaque formation. BMC Microbiol. 11, 181.

Gibbs, K.A., Isaac, D.D., Xu, J., Hendrix, R.W., Silhavy, T.J., Theriot, J.A., 2004. Complex spatial distribution and dynamics of an abundant Escherichia coli outer membrane protein, LamB. Mol. Microbiol. 53 (6), 1771–1783.

Guan, J., Shi, X., Burgos, R., Zeng, L., 2017. Visualization of phage DNA degradation by a type I CRISPR-Cas system at the single-cell level. Quant. Biol. 5 (1), 67–75.

Hendrix, R.W., 1983. *Lambda II*. Cold Spring Harbor monograph series vii. Cold Spring Harbor Laboratory, Cold Spring Harbor, N.Y, pp. 694 (3 p. of plates, 1 folded).

Hendrix, R.W., Duda, R.L., 1992. Bacteriophage lambda PaPa: not the mother of all lambda phages. Science 258 (5085), 1145–1148.

Kourilsky, P., 1973. Lysogenization by bacteriophage lambda. I. Multiple infection and the lysogenic response. Mol. Gen. Genet. 122 (2), 183–195.

Lederberg, E.M., 1951. Lysogenicity in E-coli K-12. Genetics 36 (5), 560.

Mackay, D.J., Bode, V.C., 1976. Events in lambda injection between phage adsorption and DNA entry. Virology 72 (1), 154–166.

Montag, D., Schwarz, H., Henning, U., 1989. A component of the side tail fiber of Escherichia coli bacteriophage lambda can functionally replace the receptor-recognizing part of a long tail fiber protein of the unrelated bacteriophage T4. J. Bacteriol. 171 (8), 4378–4384.

Oppenheim, A.B., Kobiler, O., Stavans, J., Court, D.L., Adhya, S., 2005. Switches in bacteriophage lambda development. Annu. Rev. Genet. 39, 409–429.

Ptashne, M., A genetic switch : gene control and phage [lambda]. 1986, Cambridge, Mass. Palo Alto, Calif.: Cell Press; Blackwell Scientific Publications. x, 128 p.

Hendrix, R.W., Casjens, S., 2006. Bacteriophage λ and its genetic neighborhood. In: Calendar, R.L. (Ed.), The Bacteriophages. Oxford University Press, Oxford, UK, pp. 409–447.

Rothenberg, E., Sepulveda, L.A., Skinner, S.O., Zeng, L., Selvin, P.R., Golding, I., 2011. Single-virus tracking reveals a spatial receptor-dependent search mechanism. Biophys. J. 100 (12), 2875–2882.

Sanger, F., Coulson, A.R., Hong, G.F., Hill, D.F., Petersen, G.B., 1982. Nucleotide sequence of bacteriophage lambda DNA. J. Mol. Biol. 162 (4), 729–773.

Shao, Q., Hawkins, A., Zeng, L., 2015. Phage DNA dynamics in cells with different fates. Biophys. J. 108 (8), 2048–2060.

Shao, Q., Cortes, M.G., Trinh, J.T., Guan, J., Balazsi, G., Zeng, L., 2018. Coupling of DNA replication and negative feedback controls gene expression for cell-fate decisions. iScience 6, 1–12.

Shao, Y., Wang, I.N., 2008. Bacteriophage adsorption rate and optimal lysis time. Genetics 180 (1), 471–482.

Szyf, M., Avraham-Haetzni, K., Reifman, A., Shlomai, J., Kaplan, F., Oppenheim, A., Razin, A., 1984. DNA methylation pattern is determined by the intracellular level of the methylase. Proc. Natl. Acad. Sci. USA 81 (11), 3278–3282.

Trinh, J.T., Szekely, T., Shao, Q., Balazsi, G., Zeng, L., 2017. Cell fate decisions emerge as phages cooperate or compete inside their host. Nat. Commun. 8, 14341.

Van Valen, D., Wu, D., Chen, Y.J., Tuson, H., Wiggins, P., Phillips, R., 2012. A single-molecule Hershey-Chase experiment. Curr. Biol. 22 (14), 1339–1343.

Wang, J., Michel, V., Hofnung, M., Charbit, A., 1998. Cloning of the J gene of bacteriophage lambda, expression and solubilization of the J protein: first in vitro studies on the interactions between J and LamB, its cell surface receptor. Res. Microbiol. 149 (9), 611–624.

Zeng, L., Golding, I., 2011. Following cell-fate in E. coli after infection by phage lambda. J. Vis. Exp. (56), e3363.

Zeng, L., Skinner, S.O., Zong, C., Sippy, J., Feiss, M., Golding, I., 2010. Decision making at a subcellular level determines the outcome of bacteriophage infection. Cell 141 (4), 682–691.